

PORE NETWORK MODEL DEVELOPMENT TO STUDY DISSOLUTION AND PRECIPITATION OF CARBONATES

Juan P. Nogués, Michael A. Celia and Catherine A. Peters[†]

Princeton University
Department of Civil and Environmental Engineering
E-201 Equad, School of Engineering and Applied Sciences NJ, 08544 USA

[†]e-mail: cap@princeton.edu

Key words: Pore network modeling, reactive transport, porosity and permeability evolution

Summary. We present the development of a reactive transport model and demonstrate its use to model the geochemical evolution of carbonate-rich pore networks within the context of geological carbon sequestration. The model's architecture is explained, as well as the equations used to model the transport of species and the kinetic and equilibrium equations used for reaction and speciation. We present model results for two scenarios, one in which calcite dissolution increases the porosity and permeability of the network and a second scenario in which calcite precipitation leads to a decrease in porosity and permeability of the network.

1 INTRODUCTION

Within the context of geological carbon sequestration, geochemical reactions between acidified brines and host formation rock or caprocks are of interest in short time scales due to the strong thermodynamic driver that acidified brines can exert on rocks containing carbonate minerals. Carbonate minerals have a buffering capacity that is able to counteract the low pH conditions from acidified brines by releasing cations to the aqueous phase. This release of ions comes at the cost of mineral phase dissolution. The dissolution of carbonates then is tied directly to a change in porosity and permeability of the host rock and consequently the ability of the host rock or caprock to effectively trap injected CO₂. This ubiquitous reaction of carbonates in the presence of acidified brines calls for a deeper exploration of the consequences these reactions might have on continuum scale properties such as porosity and permeability.

Previous works have looked at this problem by using continuum scale reactive transport models to study the effects of dissolution or precipitation of carbonates and their ability to aid in the trapping of CO₂ (such as Gherardi et al.¹). However, reactions represented at the continuum scale might misrepresent actual rates of geochemical reactions², which would lead to a misrepresentation of the porosity and permeability evolution. Therefore, in order to properly examine the reactions between acidified brines and carbonates, equations should be expressed at pore-scale because chemical potential gradients are manifested at this scale.

In this work we present a 3D reactive transport pore network model and show some of the

possible results that can be attained by such model. The objective is to be able to understand the evolution of porosity and permeability in porous media under different flow and chemical conditions as well as the impact of mineral distribution. The use of such a model can also aid in the representation of constitutive relationships, such as porosity vs. permeability curves that can be used to model larger scale processes in continuum scale models. In this particular study we focus on presenting the model architecture and the equations used to solve the transport and reactive processes. We also present the analysis of a dissolution and precipitation in a porous rock in which the minerals are uniformly distributed. We conclude with a summary of the model development and the implications of the results.

2 MODEL DEVELOPMENT

The model development followed closely the work of Li et al.² and Kim et al.³. A substantial difference is that in this model the set of mineral reactions included both fast reactions that were solved at equilibrium as well as slow reactions that were solved kinetically. Also, this model accounts for pore volume changes allowing for quantification of porosity and permeability evolution. The complete system of equations is solved sequentially by separating the reaction and transport processes in a non-iterative manner. This method was presented by Steefel and MacQuarrie⁴ [4] under the name of Sequential Non-Iterative Approach (SNIA).

The architecture of the model proceeds by first solving the pressure equation which provides the pore-to-pore fluid flows, under the assumption that steady state conditions are accurate for any given time step. Following, the model solves for 7 transport equations using an upstream weighted implicit scheme. After the concentrations have been distributed across the network, the model invokes a pore-to-pore geochemical batch reactor module that solves the equilibrium and kinetic reactions using a Newton method. Finally, after the transport and geochemistry are computed the model calls on a module that accounts for the changes in volume and pore-to-pore conductivity due to precipitation or dissolution of minerals. The flow chart depicted in Figure 1, outlines the architecture of the model as explained above.

2.1 Pore Network

We ran the model using a randomly generated pore network model based on statistics extracted from an image of a real carbonate rock. The pore network model was constructed following the algorithm proposed by Raouf and Hassanizadeh⁵. The random network was created using pore volume, connectivity and spatial distribution extracted from a synthetic μ -CT image developed by Biswal et al.⁶. Table 1 shows the continuum scale properties of the network and the mineral phase volume distribution. The pore network statistics were extracted from the μ -CT image using 3DMA-Rock⁷. For all the simulations, calcite, dolomite and kaolinite, were uniformly distributed throughout the network while anorthite and albite were randomly distributed. Quartz was considered as a non-reactive mineral in this model. Though each pore had a different volume and surface area they all had the same amount of calcite and dolomite to react with.

2.2 Reactive Species

The model considers a total of 18 aqueous species and 5 mineral species. Through the Tableau method the number of unknowns and the number of equations to be solved were reduced from a total of 23 to 8 pseudo concentrations and mole balance equations, which conserve mass and balance charge, by using a combination of 14 reaction equations.

In order to avoid issues of numerical stiffness when solving for the non-linear system of aqueous and mineral reactive species, the reaction of calcite has been set as an equilibrium reaction in the model. This was justified based on the fast rates involved with calcite minerals⁸ which drive the system of non-linear equations away from convergence unless small enough time steps are taken. The 4 kinetically controlled minerals in the model are Albite, Anorthite, Dolomite and Kaolinite.

The 8 species that result from the Tableau method are the total Carbonate-bearing species, CT, the total Calcium-bearing species, CaT, the total Magnesium-bearing species, MgT, the total Silica-bearing species, SiT, the total Aluminum-bearing species, AlT, the total Chloride-bearing species, ClT, and the total Sodium-bearing species, NaT. In our model we replace the total aqueous protons concentration, HT, by the charge balance equation in order to reduce the number of equations we solve for when considering transport.

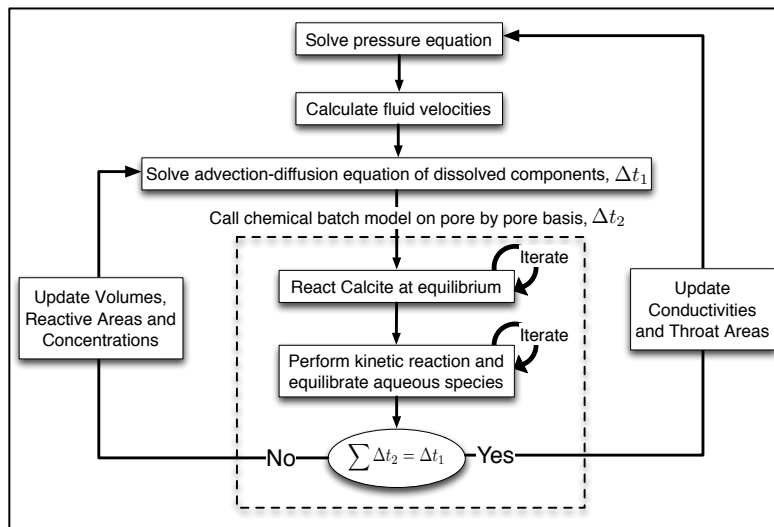


Figure 1. Flow chart explaining the model's architecture.

2.3 Pore-scale Transport and Pressure Equation

The pore-to-pore flow is defined by the Hagen-Poiseuille equation for an incompressible system, and is given by

$$\sum_{j=1}^{nc} Q_{ij} = 0 = \sum_{j=1}^{nc} C_{ij}(P_i - P_j) \quad (1)$$

where Q_{ij} is the flow rate [L^3T^{-1}] from pore i to pore j ; nc is the number of pores connected to pore i ; P_i and P_j are the fluid pressure [$ML^{-1}T^{-2}$] in pore i and j respectively; and C_{ij} is the conductivity [L^4TM^{-1}] between pores i and j .

The solute concentration is transported from pore-to-pore by advection and diffusion processes, which are modeled using the advection-diffusion equation defined at the pore scale by,

$$V_i \frac{d[\cdot]_i}{dt} = \sum_{Q_{ij}>0} Q_{ij}[\cdot]_j + \sum_{Q_{ij}<0} Q_{ij}[\cdot]_i + \sum_{j=1}^{nc} D_{ij}^* a_{ij} \frac{[\cdot]_j - [\cdot]_i}{l_{ij}} + S_{r,i} \quad (2)$$

where V_i is the volume [L^3] of pore i ; $[\cdot]_i$ represents the concentration [ML^{-3}] of a specific solute in pore i ; D_{ij}^* is the effective molecular diffusion coefficient [L^2T^{-1}] for solute $[\cdot]$; a_{ij} is the cross-sectional area [L^2] between pores i and j ; and $S_{r,i}$ is the mass rate [MT^{-1}] of change due to kinetic or equilibrium reactions with mineral phases. Through operator splitting the last term in equation (2) is not solved in conjunction with the transport of the solutes.

2.4 Equilibrium Reactions

The equilibrium reactions are represented by the mass action equation, which takes the general form

$$X_p = K_p^{-1} \gamma_p^{-1} \prod_{s=1}^{N_c} (\gamma_s Y_s)^{v_s} \quad (3)$$

where X_p and Y_s are the concentrations [ML^{-3}] of the primary and secondary component species respectively, and γ_p and γ_s are their respective activity coefficients. The equilibrium constant is represented by K_p , N_c represents the number of components and v_s is the stoichiometric reaction coefficient for a specific component species.

2.5 Kinetic Rate Laws

To solve for the evolution of the minerals that are kinetically controlled an ODE is written as which is a function of reactive surface area and a kinetic rate r . The kinetic rate r captures the rate of both dissolution and precipitation and it takes the non-linear form

$$r = \sum_j^{n_j} k_j(s)^{n_s} (1 - \Omega^m) \quad (5)$$

where k_j is the temperature dependent reaction rate constant [$\text{ML}^{-2}\text{T}^{-1}$], s is the activity of the chemical species that has a catalytic or prohibitory effect that is expressed in the exponent n_s . How far from equilibrium a specific reaction is given by Ω , which is the ionic activity product (IAP) over the equilibrium constant K_{eq} .

2.6 Network Evolution

In order to capture the changes that geochemical reactions cause on the system, we developed an algorithm-based approach to account for changes in conductivity at the pore-to-pore level due to changes in the pore body volume due to precipitation or dissolution of minerals. The algorithm is based on a series of assumptions and equations that correlate the change in volume of the pores to a change in throat diameter.

For the model in this study we have assumed that all pore throats are cylindrical in shape and have a characteristic diameter, which is used to calculate the conductivity across the pores using Equation (2). Moreover, these connecting throats are only used in the calculation of the conductivity value that feed into the pressure equation (Eq. 1) and they do not hold any volume within the system. Only pore bodies and minerals have a specified volume. We also make the assumption that any mineral precipitation or dissolution simply reduces the volume of the system and we do not take into account preferential precipitation/dissolution effects. In other words, since the pore bodies are considered as batch reactors there is no progression of geometry. As the volumes are reduced/increased, the pore throat diameter is updated using the following equation,

$$d_{ij}^{new} = d_{ij}^{prior} + d_{ij}^{prior} \cdot \left[\frac{V_i^{new} - V_i^{prior}}{V_i^{prior}} + \frac{V_j^{new} - V_j^{prior}}{V_j^{prior}} \right] \quad (6)$$

where d_{ij}^{new} and d_{ij}^{prior} are the new and prior throat diameter [L] connecting pore i and j , respectively. The difference between the new and prior values of the pore body volumes, V^{new} and V^{prior} [L^3], are used to scale the throat diameters. Equation (6) assumes that there is a direct correlation between the pore body volumes and the size of the throats connecting them.

Similarly, the reacted surface areas of the different minerals are reduced or increased when reactions occur but using a different approach. In a given pore body each mineral originally receives a different fraction of the total surface area and this fraction is scaled down or up as minerals dissolve or precipitate, respectively. The main difference is that the maximum value of the fraction of surface area is capped in order not to exceed the total available surface area. Likewise, if a mineral does not exist but it is thermodynamically favored to precipitate, the model assigns a minimal fraction of the surface area to it. It is important to note that the model does not change the total surface area but instead changes the fraction of total surface area assigned to a particular mineral. In fact, the total surface area remains unchanged.

3 RESULTS

The model was run under two conditions. The first scenario is where dissolution dominates the geochemical processes, which leads to an increase in porosity and permeability. The second scenario was run in order for carbonate precipitation to dominate the evolution of the network. In order to investigate the sensitivity of the porosity and permeability evolution we ran the two scenarios under different flow conditions by increasing the pressure difference across the system.

The first scenario results are seen in Figure 2. Figure 2 shows the co-evolution of porosity and permeability (Figure 2a) and evolution of permeability as a function of injected pore volumes (Figure 2b). The different ratios of boundary pressure (P_b) to initial pressure (P_i) create different evolutions of the permeability and porosity curves. The envelope of curves produced indicates that the permeability vs. porosity relationship is not unique but dependent on the flow conditions (i.e. highly diffusive vs. highly advective). We also see that compared to the lower P_b/P_i ratio, a high P_b/P_i ratio produces the same change in permeability with less change in porosity. This can be explained by Figure 2c, where we show the spatial average of the percent of volume change seen across the network. The flow in the network was simulated from left to right and Figure 2c shows what is the average change in pore volumes across the network for a porosity of 0.4. The change for the lowest ratio ($5e3$) is concentrated closest to the boundary while for the highest ratio ($1e5$) the changes are uniformly distributed across the network. This has to do with the advective drive. At the higher ratios (i.e. higher pressure gradients) flow is flushed across the system faster, which equates to all the pores in the network being in contact with the acidified brine. In the lower P_b/P_i ratios flow is slowly moving across the system and only the pores closest to the boundary are being reacted.

The second scenario results are shown in Figure 3. In this case water that is supersaturated with respect to calcite was flown through the system and the model described its precipitation. This created a drop in permeability and porosity. However, unlike the dissolution case, a very small change in porosity leads to a large change in permeability. For instance, a change of 0.02 in porosity (i.e. 10% change in porosity) induced a decrease in permeability of five orders of magnitude (from 10^{-15}m^2 to 10^{-20}m^2). The changes in permeability are almost instantaneous due to the fact that the water flown was supersaturated and in our model calcite can precipitate instantaneously. Most of the precipitation occurs near the face of the network next to the boundary. As the P_b/P_i ratio increases the precipitation front moves farther away from the boundary (Figure 3c) but most of the precipitation is still concentrated at the front of the network due to the decrease in permeability, which prohibits more flow through the network. It is obvious that the precipitation seen in Figure 3 is completely boundary induced and might not portray a realistic scenario. This observation indicates that simulating highly supersaturated waters in order to understand the evolution of permeability and porosity might not be the adequate way of studying the evolution of continuum scale parameters. Precipitation might have to occur by mixing induced mechanisms in order to portray a realistic scenario.

System Properties		Mineral	% by Volume
Initial Porosity [-]	0.1328	Albite	5
Initial permeability [m^2]	1.32e-15	Anorthite	5
Side of network [mm]	1.70	Calcite	10
Volume [m^3]	6.53e-09	Dolomite	60
Total number of pores	1728	Kaolinite	5
Viscosity [Pa-s]	3e-4	Quartz	15

Table 1. Pore network information and mineral distribution used in this study.

4 CONCLUSION

We have presented the development of a reactive transport model that is able to simulate the evolution of pore bodies within a network. The model can be used to understand how permeability and porosity change under different chemical (undersaturated vs. Supersaturated) and flow (advective vs. Diffusive) conditions. We simulated the evolution of permeability and porosity when both undersaturated and supersaturated waters were flown through the system. For both scenarios different pressure boundary conditions were simulated which indicated that for a particular network the evolution of the continuum scale parameters is not unique but dependent on flow conditions. For the case of the supersaturated simulations we showed that precipitation induced as a boundary condition might lead to wrong conclusions and caution should be taken when analyzing results from such simulations.

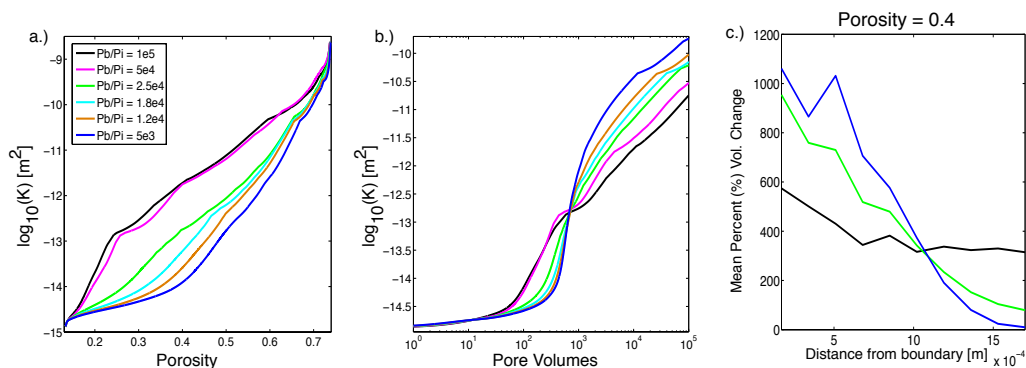


Figure 2. Porosity and Permeability (“K”) evolution as functions of each other (a) and the permeability evolution as a function of pore volumes injected (b). (c) Mean percent change in pore volume size across the network.

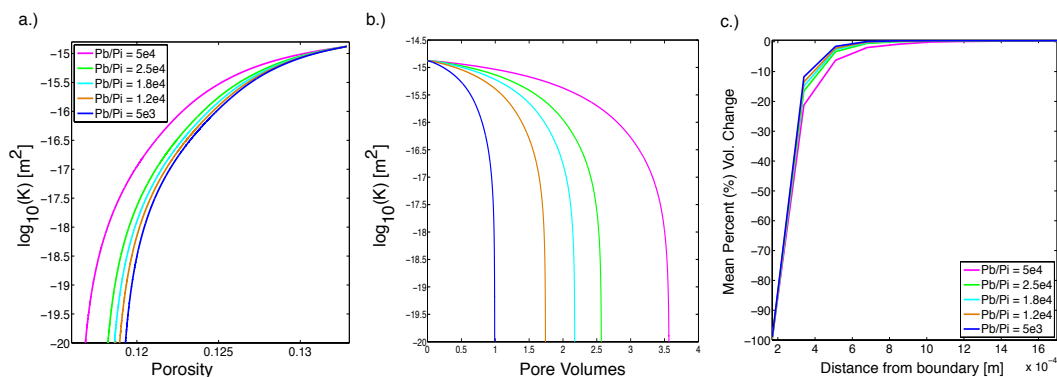


Figure 3. Porosity and Permeability (“K”) evolution as functions of each other (a) and the permeability evolution as a function of pore volumes injected (b). (c) Mean percent change in pore volume size across the network.

ACKNOWLEDGMENTS

This project was supported through funding from the U.S. Department of Energy under award number DE-FE0000749, and award number DE-FG02-09ER64748. The authors also wish to acknowledge Prof. Rudolf Hilfer from the University of Stuttgart for providing the synthetic μ -CT images of the carbonate rock, and Prof. Brent Lindquist from Stony Brook University for processing the μ -CT image using 3DMA-Rock.

REFERENCES

- [1] F. Gherardi, T.F. Xu, K. Pruess, Numerical modeling of self-limiting and self-enhancing caprock alteration induced by CO₂ storage in a depleted gas reservoir, *Chemical Geology*, 244 (2007) 103-129.
- [2] L. Li, C.A. Peters, M.A. Celia, Upscaling geochemical reaction rates using pore-scale network modeling, *Advances in Water Resources*, 29 (2006) 1351-1370.
- [3] D. Kim, C.A. Peters, W.B. Lindquist, Upscaling geochemical reaction rates accompanying acidic CO₂-saturated brine flow in sandstone aquifers, *Water Resources Research*, 47 (2011) W01505.
- [4] C. Steefel, K.T.B. MacQuarrie, Approaches to Modeling of Reactive Transport in Porous Media, in: P.C. Lichtner, C. Steefel, E.H. Oelkers (Eds.) *Reactive Transport in Porous Media*, Mineralogical Society of America, Washington D.C., 1996.
- [5] A. Raouf, S. Hassanizadeh, A New Method for Generating Pore-Network Models of Porous Media, *Transport in Porous Media*, 81 (2010) 391-407.
- [6] B. Biswal, R.J. Held, V. Khanna, J. Wang, R. Hilfer, Towards precise prediction of transport properties from synthetic computer tomography of reconstructed porous media, *Physical Review E*, 80 (2009).
- [7] W.B. Lindquist, S.M. Lee, D.A. Coker, K.W. Jones, P. Spanne, Medial axis analysis of void structure in three-dimensional tomographic images of porous media, *Journal of Geophysical Research*, 101 (1996) 8297 – 8310